scientific reports

Check for updates

OPEN

A muscle synergy-based method to improve robot-assisted movements

María Alejandra Díaz[1,2]✉, Parham Haji Ali Mohamadi[2,3], Sander De Bock[1,2], Kevin Langlois[2,3], Joris De Winter[2,4], Tom Verstraten[2,4] & Kevin De Pauw[1,2]✉

There is increasing interest in using assistive robotic devices to support motor re-learning and recovery in individuals with neurological impairments. These robots aim to enhance overall motor control by providing adaptive assistance. However, using muscle synergies in designing control strategies for rehabilitation devices remains an emerging area of research. This study proposes a novel synergy-based objective function to assess how changes in robotic assistance levels affect muscle synergies in a 2D reaching task in the horizontal plane. Healthy participants performed the task in a transparent mode and with three levels of assistance while holding a weight. EMG signals from seven muscles were decomposed into muscle synergies across all conditions. First, we defined the three reference synergies as baseline knowledge of the synergies required to execute the task and their modulation, resulting in three main muscle recruitment strategies across ten participants. We then introduce three metrics to assess variations in motor coordination relative to the reference synergies. These metrics assessed how closely participants' muscle activation patterns matched the reference synergies, capturing variations in the shape, timing, and overall similarity of the muscle activation profiles. Finally, by combining the metrics, we present an objective function that assesses participants' motor coordination when performing the task with the added weight. The results highlight the importance of personalized assistance, as not all individuals could closely match the reference synergies with the same level of assistance. Additionally, the objective function demonstrated statistically significant differences in performance across assistance levels. Although this is a preliminary study, it presents promising results as a first step towards implementing human-in-the loop optimization in robotic-assisted rehabilitation.

Recent advances in assistive robotics have focused on improving human-robot interaction to enhance motor control, biomechanics, and user performance across various movement tasks[1]. Additionally, research on robotic assistance has also examined the role of the central nervous system (CNS) in coordinating and controlling muscle contractions[2,3]. While executing a movement may appear simple, the control behind it involves a high degree of complexity[2]. Then, the CNS is responsible for adjusting and fine-tuning muscle activation into task-specific groups known as muscle synergies, which make coordinated movement across different movements possible[3,4]. The muscle synergies help simplify motor control and allow the study of muscle coordination patterns under various conditions[5], including robotic assistance. Thus, understanding how the CNS regulates the dynamic behavior and redundancy of the musculoskeletal system could lead to better motor control assessment even when robotic devices assist a movement under challenging conditions.

Muscle synergy analysis decomposes electromyography (EMG) activation patterns into time-varying signals and a matrix of weights, also known as synergy vectors[6]. Linearly combining the synergy signals and the weights produces a synergy-reconstructed muscle activation pattern and a reconstruction error[1]. This error decreases as more synergies are extracted[7]. Studies have demonstrated that a small set of synergies can account for over 90% of the variance (VAF) in muscle activity across upper-limb tasks, with these synergies being consistent across different individuals [8]. In other words, selecting an appropriate number of muscle synergies can explain at least 90% of muscle activity, effectively reducing the dimensionality and complexity of the EMG signals.

The application of muscle synergies extends to robotic assistance, where they are used to improve rehabilitation outcomes. This approach explores the robot's role in motor relearning and its impact on human-robot interaction[9,10]. Incorporating muscle synergies in the design of robotic assistance device control strategies can positively influence motor control and coordination in neurological patients. For example, Scano et al.[9] analyzed the impact of robotic assistance during 3D-reaching movements in stroke patients, within the context of muscle synergies. Their findings suggest that interaction with the robot promoted the emergence of

[1]Human Physiology and Sports Physiotherapy Research Group, Vrije Universiteit Brussel, Brussels 1050, Belgium. [2]Brussels Human Robotics Research Center, Vrije Universiteit Brussel, Brussels 1050, Belgium. [3]IMEC, Leuven 3001, Belgium. [4]Robotics and Multibody Mechanics Research Group, Flanders make, Brussels 1050, Belgium. ✉email: ma.diaz@vub.be; kevin.de.pauw@vub.be

physiological-like synergies, potentially enhancing motor relearning. Similarly, Afzal et al.[11] investigated muscle synergies during exoskeleton-assisted walking in patients with multiple sclerosis. Their study highlighted the relevance of this analysis in providing meaningful clinical insights into motor deficits. Furthermore, synergies have also been used in robotic assistance optimization[12,13] and to reconstruct EMG signals from a pathological population using synergies from healthy individuals[7].

In the context of optimizing robotic assistance, recent research has been working towards human-in-the-loop optimization (HILO)[14]. This methodology automatically and continuously updates control parameters that define the assistance based on the user's response to changes in control characteristics to maximize the user's performance[14]. A cost function, or objective function, is essential to quantitatively measure users' response to the robot's assistance. Studies have shown that quantifying human physiological signals and neuromuscular control, and incorporating this information into the robot's feedback loop through iterative optimization, can help identify assistance settings that are tailored to the user's needs[14]. These optimized settings can significantly improve users motor coordination and enhance performance during human-robot interaction[12].

This research aims to develop a synergy-based objective function to understand how varying levels of assistance from an assistive robot affect muscle synergies in 10 healthy participants. Specifically, it will demonstrate how changes in assistance influence participants' ability to perform a 2D reaching task under challenging conditions (i.e. holding an added weight) (Fig. 1), impacting their motor control and coordination. The conditions tested include 1) a transparent mode and 2) three levels of assistance while holding an added weight. We constructed a set of reference synergies by clustering the muscle synergies extracted during the task in transparent mode. These reference synergies serve as a baseline to understand typical task execution and provide a comparative structure for analyzing synergy variations when external assistance is introduced. Using these reference synergies, we then assessed how muscle synergies altered when participants completed the task with added weight and varying levels of assistance. We hypothesize that a well-defined objective function can assess changes in motor control during these challenging and assisted tasks and identify optimal settings that align participants' control with the reference synergies. The results of this research could improve rehabilitation strategies using assistive robotic devices, as muscle synergies could reveal precise alterations in motor control compared to traditional clinical assessments[15,16].

Results

Reference synergies

For each participant and each trial, we extracted 3 muscle synergies, which was sufficient to get a *VAF* higher than 0.9 (Supplementary Fig. S1). We identified three reference synergies (Fig. 2). The first and third synergy show how crucial the deltoid muscles are in moving the arm away from the body. The deltoid anterior leads the motion when reaching in a straight line from point A to point B. Moving from point A to point C requires coordinated activation mainly from the deltoid medial and deltoid posterior but also from the triceps. The triceps muscle is essential in extending the elbow, while the deltoid muscles are responsible for externally rotating and abducting the shoulder, enabling diagonal arm movements.

Figure 3 shows the results of the K-means clustering algorithm, which grouped all the synergy vectors into three different clusters. In the heat map, normalized muscle activation levels are color-coded, with yellow representing higher activation and blue representing lower activation. Each cluster contains synergies with similar muscle contributions. The centroid of each cluster was calculated and used as the reference muscle synergy. The 60 synergy vectors were derived from 20 trials conducted by 10 participants under two conditions: transparent mode (one trial per participant) and with no weight and low support (one trial per participant). Three muscle synergies were extracted from each trial. Of these trials, 70% contained all three reference synergies, while 30% included only two.

The supplementary material provides the calculated muscle synergies of all participant's executing the task in transparent mode (Supplementary Fig. S2) and with no weight and low assistance (Supplementary Fig. S3). In

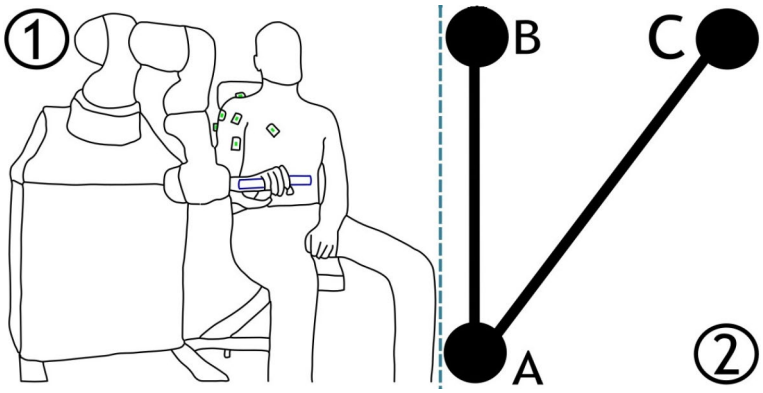

Fig. 1. (1) A participant with the KUKA LBR Med 14 executing a 2D reaching task while holding a weight. (2) The 2D reaching task. Participants had to reach first in a straight line (from A to B), then in a 45-degree angle (from point A to C).

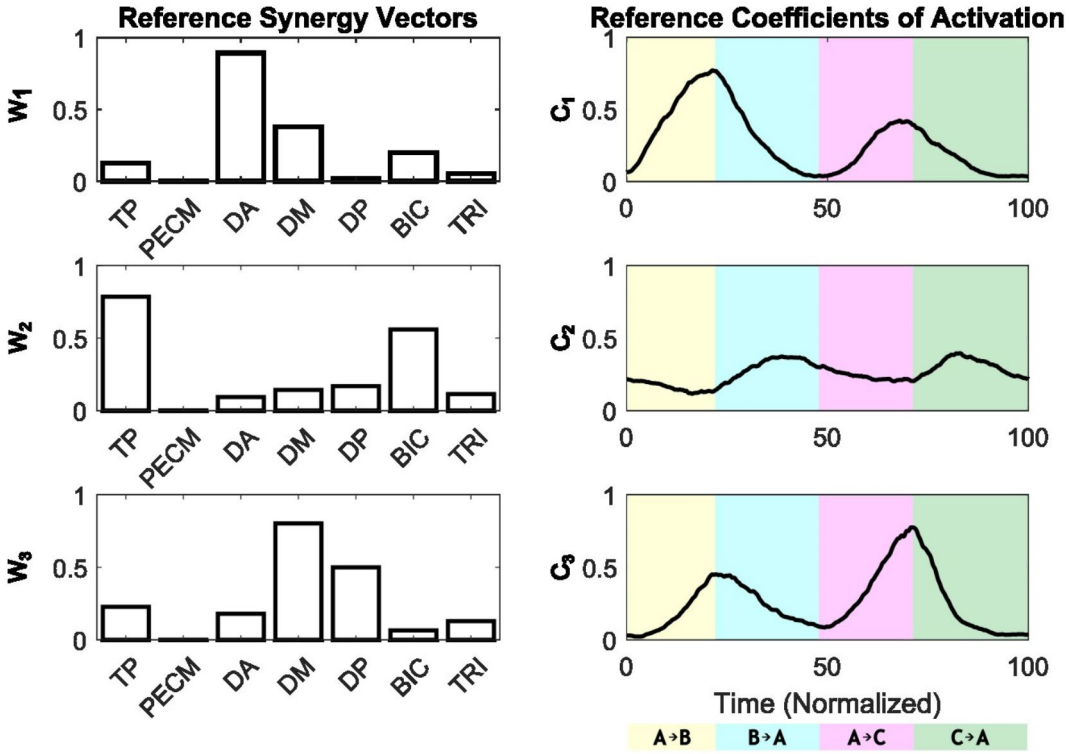

Fig. 2. The three reference synergies that describe the task in participants. In the left panel the synergy vectors (W_i) from the K-means algorithm. In the right panel the dynamic activation coefficients ($C_i(t)$) represent mean trajectories across all subjects for the corresponding synergy weights shown on the left panel. The color coding on the right panel corresponds to different phases of the 2D reaching task outlined in Fig. 1, with each color indicating a specific trajectory between points..

addition, extended details of how each synergy cluster corresponds to individual participants (Supplementary Fig. S4) based on the K-means cluster.

Comparison between assisted and reference muscle synergies

We calculated the cross-validated variance accounted for (CV_{VAF}) to evaluate the quality of the estimated vectors. Trials with a negative CV_{VAF} were excluded from the analysis. As a result, 4 out of 30 trials, belonging to participants 1 and 4, were removed. Thus, the final analysis includes data from 8 participants.

Figure 4 presents the total Euclidean distance (TED) between the estimated activation coefficients (C_{est}) and the reference coefficients (C_{ref}), as well as the total absolute difference between the estimated synergy vectors (W_{est}) and the reference vectors (W_{ref}). This figure provides a comparative visualization of the behavior of these variables for 8 participants across the three assistance levels.

As shown in Fig. 4, the metrics proposed to assess the C_{est} and W_{est} provide similar trends for most participants, suggesting consistent adaptations across synergy modulation (via C) and synergy composition (via W). Participants 3, 6, 8, and 10 show similar behavior in both the *TED* (blue line) and the total absolute difference (*TAD*) (orange line) metrics, indicating a coordinated response in synergy modulation and composition.

In contrast, participants 2, 5 and 7 have noticeable differences between the behaviors represented by the blue and orange lines, indicating different responses in synergy modulation versus composition. For these participants, calculating C_{est} and comparing it with C_{ref} did not show satisfactory results, as no clear minimum was observed. This could be attributed to variability in their muscle activation patterns. However, the absolute difference metric (W_{est} compared to W_{ref}) shows better results for participants 2 and 7, indicating a more reliable adaptation in synergy composition even when modulation patterns vary.

Additionally, Table 1 displays the correlation between the synergy similarity (*SSV*), *TAD*, *TED*, providing a quantitative comparison of these metrics. As expected, a strong negative correlation (> 0.9) is observed between *TAD* and *SSV*. This relationship indicates that a higher synergy similarity corresponds to a smaller difference between W_{est} and W_{ref}, leading to a lower *TAD*. This result is anticipated as both metrics are derived from the same processing method. Even though the correlation between *TED* and *TAD* is moderate (around 0.5), there is a clear positive trend. A similar result is observed between *TED* and *SSV* (> 0.6).

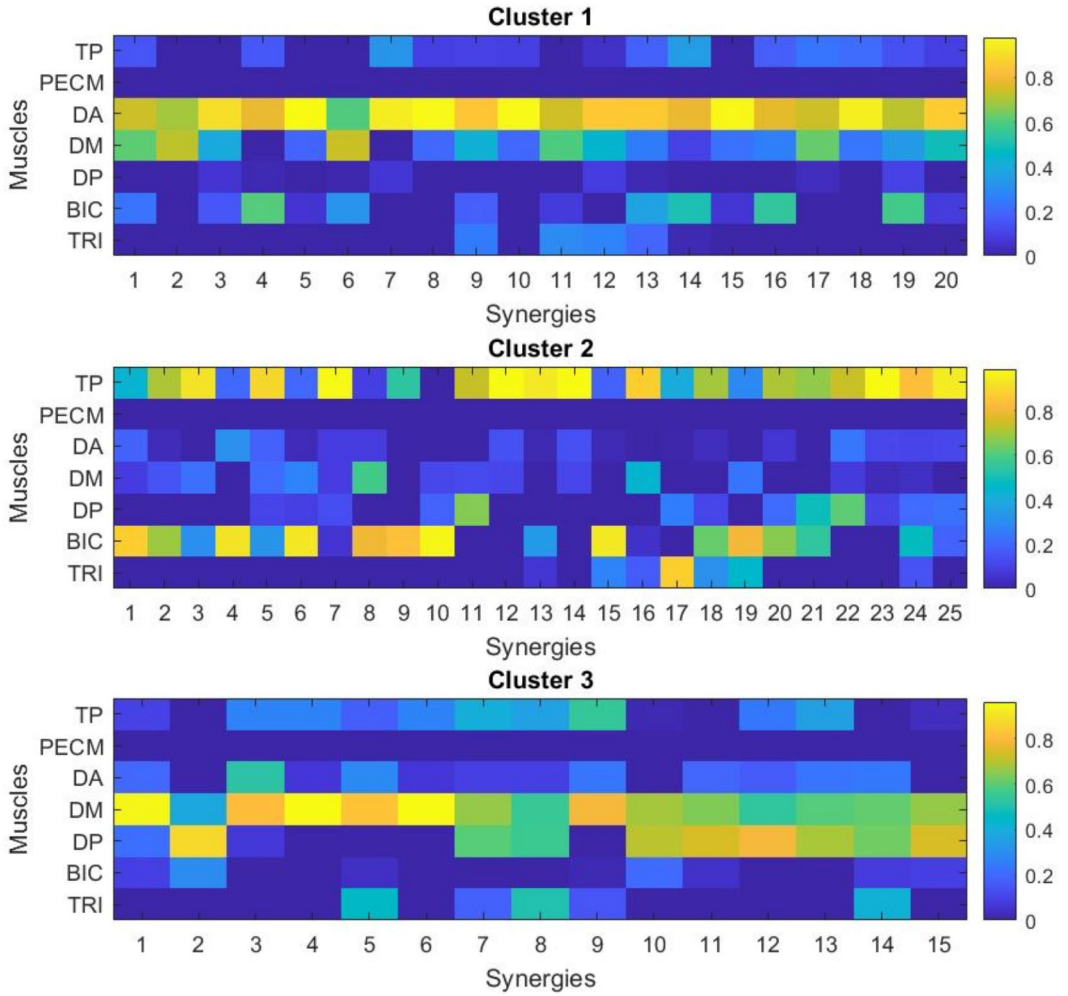

Fig. 3. Heat-maps of the K-means clusters. Each heat-map represents one of the three clusters, with the y-axis indicating the muscles (TP, PECM, DA, DM, DP, BIC, TRI) and the x-axis representing the synergy vectors. The color scale indicates the activation level for each muscle within a synergy vector (yellow = high activation, blue = low activation).

Muscle-synergy based objective function

The results of optimized weight combinations using PSO were $g_1 = 1.4$ and $g_2 = -0.28$. Table 2 presents the cost function (CF) outputs for each participant across the different assistance levels. The lowest CF values, highlighted in blue, indicate the highest similarity to the reference synergies.

For participants 3, 5, 8 and 9 the maximum assistance level resulted in the lowest CF output, suggesting that higher assistance was more effective in facilitating the desired motor control. In contrast, for participants 2, 7 and 10 the lowest assistance level produced the best outcome. In this case, providing more assistance might reduce engagement and hinder the modulation of synergies.

Interestingly, participants with lower CF minima have prior experience with assisted movement. This familiarity may allow them to adapt more readily to assistance, as reflected in their generally lower CF values. For instance, participant 8, with the lowest CF minimum at 9.84, may efficiently integrate assistance into their movement patterns, requiring minimal synergy restructuring to achieve the desired activation. In contrast, participants with limited prior experience, such as participant 2 (whose minimum CF is 14.23), may exhibit higher CF values. This difference suggests that they undergo more significant adjustments in muscle synergies or activation strategies in response to assistance.

Discussion

In this study, we proposed an objective function designed to improve motor control by quantifying how closely the user's muscle synergies align with a set of reference synergies during a 2D reaching task. This function evaluates changes in the structure of muscle synergies in response to varying levels of assistance during a challenging task. It provides a quantitative framework that identifies the optimal level of assistance to achieve the desired motor coordination. Moreover, we introduced a method to evaluate motor coordination using our defined reference synergies as a baseline for comparison. Our future goal is to apply this approach to pathological populations

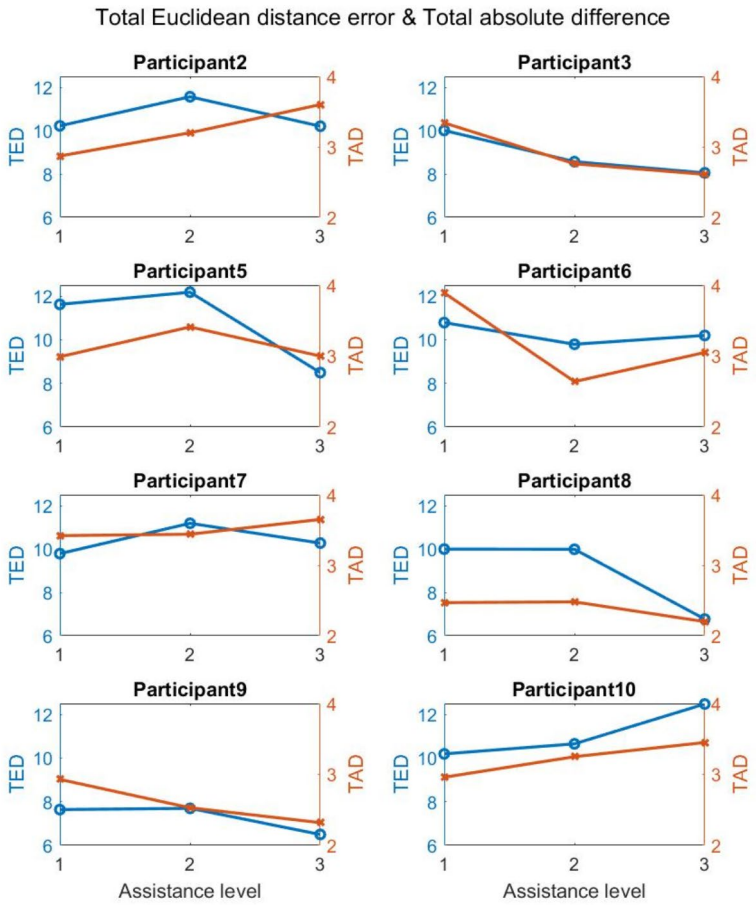

Fig. 4. Comparison of Total Euclidean distance error (TED, in blue) between C_{est} and C_{ref}, and the total absolute difference (TAD, in orange) between W_{est} and W_{ref} across three assistance levels; 1 = low, 2 = mid, 3 = high.

	TAD	Total SSV	TED
TAD	1.00	− 0.94*	0.53*
Total SSV	− 0.94*	1.000	− 0.63*
TED	0.53*	− 0.63*	1.00

Table 1. Correlation coefficients between TAD, total SSV and TED.* indicates a significance level of $p < 0.01$.

	Low assistance	Mid assistance	Max assistance
Participant 2	**14.23**	16.04	15.24
Participant 3	14.68	12.43	**11.70**
Participant 5	15.80	16.94	**12.69**
Participant 6	16.22	**13.48**	14.46
Participant 7	**14.57**	15.99	15.38
Participant 8	13.44	13.45	**9.84**
Participant 9	11.74	11.23	**9.74**
Participant 10	**14.33**	15.20	17.30

Table 2. Objective function output for all participants. For each participant, the lowest objective function values are highlighted in bold, indicating the highest similarity to the reference synergies.

using muscle synergies, which have been proposed as physiological biomarkers to assess the pathological state of the motor system in different patients[15]. This could allow us to tailor robotic rehabilitation strategies to address specific deficits in motor control and coordination, ultimately enhancing the effectiveness of therapy.

Although *SSV* and *TED* are two metrics that have already been used in previous studies to compare muscle synergies variations[1,17], evaluate the effect of robotic assistance on muscle coordination[3,18] and assess different patient populations[19]. This study introduces a novel cost function that combines *SSV* and *TAD* to explore muscle synergy adaptation and provide deeper insights into motor coordination. Specifically, by comparing synergy vectors (W_{est}) with reference synergies (W_{ref}), the function quantifies how W_{est} must adapt to maintain stable activation patterns. This function highlights the flexibility and adaptability of muscle synergies in response to robotic assistance and challenging conditions.

The differences in trends across participants suggest that the CNS adjust to task demands (e.g., added weight or assistance) either by adjusting synergy activation timing (through *C*) or by altering the synergy structure (through *W*). Figure 4 suggests that participants showing similar trends may have a CNS that adapts with a balanced approach, adjusting both *W* and *C* in coordination to meet task requirements. In contrast, participants with different trends rely more on specific changes in either activation timing or muscle grouping.

Even though, the criteria for determining ”good” or ”bad” outputs from the proposed cost function remain unclear, which is a limitation from this study, we believe that the personalized nature of these outputs, which vary within participants across different levels of assistance, indicates that our approach is promising. Results demonstrated that not all individuals can effectively replicate the reference synergies with the same level of assistance, indicating the need for personalized support. The variability in CF minimums and optimal assistance levels across participants confirms that individualized assistance best enables each person to replicate the reference synergies, even with added weight. Our optimization framework accounts for this personal variation, addressing motor adaptation's complex and individualized nature. As Ting et al.[20] emphasize, individualization is essential to promote active engagement during therapy. Patients who receive assistance that is too high or too low may not be sufficiently challenged, potentially hindering their progress. This approach could enhance rehabilitation by tailoring assistance to each person's unique motor patterns, optimizing relearning and functional improvements, and preventing compensatory strategies that could hinder long-term recovery[2,20].

Regarding optimizing human-robot interaction, our findings suggest that integrating quantified neuromuscular control into robot feedback can enhance motor control and engagement during robot-assisted movements. This conclusion is drawn from the observed adaptability of muscle synergies to varying levels of robotic assistance, as quantified by the changes in the output of the proposed cost function. The results demonstrate that different assistance levels influence both the structure of muscle synergies and their activation patterns, highlighting the potential of personalized feedback to optimize motor coordination. This approach effectively captures the main components of human-in-the-loop optimization[14] by integrating metrics that assess muscle synergies through a cost function and an optimal value that minimizes that function during a robot-assisted task[12]. This combination allows for real-time adjustments of assistance based on the user's neuromuscular performance, ensuring the support is adaptive and personalized. As a result, this framework could offer a more rational and targeted form of assistance, presenting a novel and feasible approach that could be used in rehabilitation strategies to improve patient outcomes. Ultimately, understanding the effect of assisted movements on muscle activity and motor synergies will help optimize the use of robotic devices in rehabilitation[2,10].

This study represents an initial step towards implementing HILO in robotic-assisted rehabilitation. To further improve the research study, additional data from more participants will help refine the reference synergies, and testing on more complex tasks will allow us to better evaluate the performance of our objective function. Ultimately, validating this approach in patient populations will help establish its effectiveness compared to conventional therapy and further advance individualized rehabilitation strategies. The final goal is to enhance individualized therapy and better track rehabilitation progress.

Methods

This study followed the standards of the Declaration of Helsinki, and the local ethical commission (Vrije Universiteit Brussel and UZ Brussel) granted ethical approval (B.U.N. 1432022000180). Participants provided written informed consent prior to the study.

Experimental setup

The KUKA LBR Med 14 (KUKA, Augsburg, Germany) is a collaborative robot specifically designed for medical applications that involve human-robot interaction (see Fig. 1-Left). This robotic arm features 7 degrees of freedom and can be programmed through demonstration, which facilitates efficient task replication. The process begins with an operator demonstrating a movement task to the robot, while the subject's arm is connected to the robot's end-effector via a physical human-robot interface. During this demonstration, the robot remains ”transparent” to the movement. This physical interface is engineered to ensure effective force transmission between the subject's arm and the robot's end-effector, promoting safe and comfortable interactions[21].

Once the robot has recorded the movement, it can replicate the task. To enhance the robot's control and adaptability, we utilize a Proxy-Based Sliding Mode Controller[22]. This controller allows the robot to respond compliantly when an external force exceeding a certain threshold is applied to the end-effector, such as during contact with the environment or a human operator. This feature improves the robot's safety and robustness in dynamic settings[22]. It enables the operator to define the maximum force that can be applied at the robot's end-effector, while still allowing the subject to deviate from the recorded trajectory.

In this context, setting a lower force threshold translates to a lower robot's assistance level for tracking the trajectory and completing the recorded task. For example, when the robot operates with a low assistance level (20*N*) and the subject does not follow the recorded trajectory, the robotic arm exerts only 20*N* of force to guide

the subject's arm back to the trajectory. In this experiment, we considered a transparent mode (where the robotic arm exhibits minimal resistance to external forces) and three levels of assistance: low = 20*N*, mid = 100*N* and high = 200*N*.

Experimental protocol

Ten healthy male participants (age = 26.7 ± 3.8 *years*, body mass = 66.5 ± 8.5 *kg*, height = 173.4 ± 4.8 *cm*) sat on a chair and positioned their arms on the cuff. We explained the 2D point-to-point reaching task, both in a straight line and at a 45-degree angle (Fig. 1-Right). Following the explanation, participants were guided through the task (as detailed in the experimental setup for safety), and the trajectory was recorded. Subsequently, participants were allowed to perform the task multiple times at varying assistance levels to familiarize themselves with the robot.

Before starting the experimental test, 7 EMG sensors (Trigno surface electromyography system, Delsys Inc., Natick, MA, USA) were located on upper limb muscles: Upper trapezius (TP), pectoralis major (PECM), Deltoid anterior (DA), Deltoid medial (DM), Deltoid posterior (DP), Biceps brachii (BIC) and Triceps brachii (TRI). During the experimental trial, participants performed 10 repetitions of the task with the robot in transparent mode. The participants then performed the task 10 times without weight and with low assistance. Finally, participants performed the task 10 times while holding a weight of 3*kg* with one hand (i.e. the hand from the arm that was assisted by the device). The reasoning to ask participants to perform the task with this weight is to add a challenging condition and be able to assess the effect of assistance. This task was carried out with three assistance levels: low, medium and high assistance. Rest periods were allowed between transitions between assistance levels. The experiment lasted approximately 60 minutes.

Data analysis

We first constructed a pool of muscle synergies (reference synergies) using the trials where participants executed the task in transparent mode and without weight and low assistance. These synergies represent the muscle combinations that healthy participants need to perform the 2D task even with a low help from the robot. Afterwards, we calculated the muscle synergies when participants wherfe holding the weight with three assistance levels and compare them with the reference synergies. Adding a weight increased the difficulty of the task, demanding additional effort and leading to muscle compensations that altered the muscle synergies. Our objective was to demonstrate how assistance could help guide participants with altered muscle synergies (resulting from the added weight) back towards the reference synergy patterns.

EMG processing

The EMG signals were preprocessed before decomposing them into muscle synergies, following the steps outlined below. Raw EMG signals were filtered offline with a sixth-order Butterworth band pass filter between 30 and 400 Hz, subsequently full-wave rectified, and low-pass filtered (6 Hz) using a sixth-order Butterworth filter. For each participant and muscle, the resulting linear envelopes were normalized with respect to the maximum peak amplitude of each muscle. The latest was selected as the maximum value of a 50 ms moving-average window applied to the muscle linear envelopes in each trial[23,24]. Then, we further processed the EMG signal to extract muscle synergies.

Reference synergies

For each participant, we extracted the muscle synergies from the mean EMG of the last four repetitions of the task in transparent mode using a non-negative matrix factorization (NNMF), previously used for muscle synergy analysis[6,25,26]. NNMF breaks down muscle activities represented by EMG signals into a linear combination of fixed synergy vectors (W_i) and dynamic activation coefficients ($C_i(t)$). The synergy vectors represent how much each muscle contributes to a specific synergy (*i*), while activation coefficients capture temporal changes. Multiplying the synergy vectors by $C_i(t)$ allows the reconstruction of EMG signals, as outlined in Eq. (1). To assess how well we can reconstruct the EMG data by combining modules and activation coefficients we used a metric called variance accounted for (VAF). The VAF explains how well we can reconstruct the EMG data by combining modules and activation coefficients. We targeted a VAF of more than 0.9[1], indicating more than 90% data reconstruction. VAF was calculated as described in[8,17].

$$\boldsymbol{EMG}_{signals}(t) \approx \sum_{i}^{N_{syn}} \boldsymbol{C}_i(t)\boldsymbol{W}_i \tag{1}$$

Then, we identified a set of spatial and temporal modules that compactly describe the EMG activity during the trial across all participants. These modules effectively represent the muscle activity patterns of healthy participants for this experimental task. To identify the reference muscle synergies, we performed a clustering analysis using the K-means algorithm, similar to the approach by Jeong et al.[1]. K-means is a clustering method that groups similar observations into clusters. In this case, it grouped the synergy vectors from all participants into three distinct clusters, as all participants consistently exhibited three muscle synergies (with $VAF > 0.9$). We used the squared Euclidean distance to determine the centroid of each cluster. As a result, we obtained the reference synergy vectors (W_{ref}). Finally, to calculate C_{ref}, we grouped all the synergy activation coefficients associated with each cluster-specifically, those corresponding to the synergy vectors grouped within the same cluster during the K-means analysis-and calculated their mean on a point-by-point basis.

Assisted synergies compared to reference synergies

As in our previous study[27], this study aimed to understand how performing the task with added weight and three different levels of assistance affects muscle synergies. In the earlier study[27], we assumed that the reference synergy vectors (W_{ref}) represent fundamental building blocks of movement that remain relatively unchanged across conditions, with variations expected primarily in the temporal activation of these synergies. This approach serves as a way to explain how the CNS adjusts synergy activation under different conditions, such as added weight or varying levels of assistance.

In the current study, we first followed the same method as in our previous work[27] to estimate the activation coefficients (C_{est}) from a trial using the reference synergy vectors (W_{ref}). Then, we calculated the difference between C_{est} and C_{ref} at each time point using the Euclidean distance (*ED*). This strategy allows us to assess how the reference synergies (W_{ref}) were modulated during a trial based on the measured EMG signals. For each participant and assistance level, we calculated a total Euclidean distance (*TED*) by summing the *ED* from each synergy.

In addition, we introduced a second method. In this case, we assumed that the activation patterns required to perform the task (C_{ref}) remain stable, even under different conditions. Next, we estimated the synergy vectors (W_{est}) for each trial using the C_{ref} and Eq. (2). This estimation comes from rearranging Eq. (1) to solve for W_i , and C_i was replaced by C_{ref}.

$$\boldsymbol{W}_{est} = [\boldsymbol{C}_{ref}^{\top}\boldsymbol{C}_{ref}]^{-1} \cdot [\boldsymbol{C}_{ref}^{\top} \cdot \boldsymbol{EMG}_{signals}(t)] \tag{2}$$

To evaluate changes between W_{est} and W_{ref}, we calculated the absolute difference per muscle for each synergy. This method allowed us to understand how the synergy vectors (W_{est}) needed to adapt to achieve the activation patterns from the reference synergies. We calculated two metrics for each participant and assistance level. First, we computed the total absolute difference (*TAD*) by summing the absolute differences across muscles and synergies ($TAD = \sum |W_{est} - W_{ref}|$). Second, we calculated the synergy similarity vector (*SSV*) between synergy vectors, and then the values were summed to construct a total *SSV*. The *SSV* is a commonly used method to compare synergy vectors[1,17,19]. Typically, Eq. (3) is used, where W_i^k and W_j^k represent the *k*th synergy vectors from the *i*th and *j*th trials, respectively.

$$SSV\left(W_i^k, W_j^k\right) = \frac{W_i^k \cdot W_j^k}{\left\|W_i^k\right\|_2 \cdot \left\|W_j^k\right\|_2} \tag{3}$$

After estimating both W_{est} and C_{est} we assessed the quality of reconstruction (i.e. the quality of the estimated vectors) using the cross-validated VAF (CV_{VAF})[28] as:

$$CV_{VAF} = 1 - \frac{\sum (X_i - W_{est}C_i(t))^2}{\sum \left(X_i - \overline{X_i}\right)^2} \tag{4}$$

where X_i is the original data (i.e. $EMG_{signals}$), $\overline{X_i}$ is the mean of the original data, and $W_{est}C_i(t)$ is the reconstructed data using the estimated synergy matrix W_{est} and the calculated coefficient matrix from X_i. If CV_{VAF} is close to 1, it means that W_{est} and $C_i(t)$ are able to accurately reconstruct the original EMG data. This suggests that W_{est} provides a good representation of the actual muscle synergies in X_i, closely aligning with the reference synergies W_{ref}. Trials with a negative CV_{VAF} were excluded from the analysis.

Finally, we compared the results of both methods to assess how different the two perspectives are in explaining muscle synergies under the tested conditions.

Muscle-synergy based objective function

The goal was to construct a synergy-based objective function to optimize user-cobot interactions under varying levels of robotic assistance. Using task-related muscle synergy metrics, such as *SSV* and *TAD* from trials where participants carried weights across three assistance levels, we designed the objective function as follows:

$$CF = g_1 * TAD + g2 * SSV \tag{5}$$

where, g_1 and g_2 are the variables weight to be optimized. When optimizing the weights, we first set the ranges of weights: $g_1 \in [1, 2]$ and $g_2 \in [-1, 0]$ to ensure that the cost function captures the trade-off between the two variables. Given the negative correlation between *TAD* and *SSV* we set g_2 to balance their opposing trends. This setup enhances the contrast between different assistance levels, favoring conditions with lower *TAD* and higher *SSV*.

The aim was to achieve a significant difference between the CF output (see Eq. (5)) across the different assistance levels. Accordingly, we designed the optimization of the objective function with a statistical focus to obtain the optimal weights combination. We expressed the cost function as a matrix:

$$J_m = [g_1 \quad g_2] * \begin{bmatrix} SSV_{11} & SSV_{12} & SSV_{13} & \dots & SSV_{n1} & SSV_{n2} & SSV_{n3} \\ TAD_{11} & TAD_{12} & TAD_{13} & \dots & TAD_{n1} & TAD_{n2} & TAD_{n3} \end{bmatrix} \tag{6}$$

where J_m is a 1*x*27 vector that was then reshaped to an *nx*3 matrix, representing each participant's *n* cost function across the three assistance levels. We calculated the differences across the levels of assistance and used the Kruskal-Wallis test to maximize statistical differences. The p-value from this non-parametric test served as

the objective function output. Finally, we used a particle swarm optimization (PSO) to minimize the p-value to obtain the optimal weight combination for g_1 and g_2. The PSO was run in MATLAB using the *particleswarm* function, the swarm size and maximum iteration number were set to 30 and 50 respectively[29].

Finally, we developed a user-friendly graphical interface (see supplementary material) designed to assess the similarity between a given task and a set of reference synergies. This tool enables the comparison of both temporal and spatial activations, as well as the evaluation of the cost function output. Additionally, it incorporates a gradient descent optimization strategy, allowing users to perform HILO optimization when needed. This feature helps determine the optimal level of assistance required to achieve the desired motor control for the task.

Data availibility

The datasets generated during the current study are available from the corresponding author on reasonable request.

Received: 9 November 2024; Accepted: 2 March 2025
Published online: 04 April 2025

References

1. Jeong, H. et al. Muscle coordination and recruitment during squat assistance using a robotic ankle-foot exoskeleton. *Sci. Rep.* **13**, 1363 (2023).
2. Torricelli, D. et al. Muscle synergies in clinical practice: Theoretical and practical implications. *Emerging Therapies in Neurorehabilitation II* 251–272 (2016).
3. Cancrini, A. et al. The effects of robotic assistance on upper limb spatial muscle synergies in healthy people during planar upper-limb training. *PLoS ONE* **17**, e0272813 (2022).
4. Oshima, A., Nakamura, Y. & Kamibayashi, K. Modulation of muscle synergies in lower-limb muscles associated with split-belt locomotor adaptation. *Front. Hum. Neurosci.* **16**, 852530 (2022).
5. d'Avella, A. et al. Modularity in motor control: from muscle synergies to cognitive action representation (2015).
6. Lee, D. D. & Seung, H. S. Learning the parts of objects by non-negative matrix factorization. *Nature* **401**, 788–791 (1999).
7. Rabbi, M. F. et al. A muscle synergy-based method to estimate muscle activation patterns of children with cerebral palsy using data collected from typically developing children. *Sci. Rep.* **12**, 3599 (2022).
8. Scano, A. et al. A comprehensive spatial mapping of muscle synergies in highly variable upper-limb movements of healthy subjects. *Front. Physiol.* **10**, 1231 (2019).
9. Scano, A. et al. Effect of human-robot interaction on muscular synergies on healthy people and post-stroke chronic patients. In *2017 International Conference on Rehabilitation Robotics (ICORR)*, 527–532 (IEEE, 2017).
10. Coscia, M., Tropea, P., Monaco, V. & Micera, S. Muscle synergies approach and perspective on application to robot-assisted rehabilitation. In *Rehabilitation Robotics*, 319–331 (Elsevier, 2018).
11. Afzal, T. et al. Evaluation of muscle synergy during exoskeleton-assisted walking in persons with multiple sclerosis. *IEEE Trans. Biomed. Eng.* **69**, 3265–3274 (2022).
12. Ma, Y. et al. Optimizing exoskeleton assistance: Muscle synergy-based actuation for personalized hip exoskeleton control. In *Actuators*, vol. 13, 54 (MDPI, 2024).
13. Hamaya, M. et al. Exploiting human and robot muscle synergies for human-in-the-loop optimization of EMG-based assistive strategies. In *IEEE Int. Conf. Robot. Autom.*, 549–555 (IEEE, 2019).
14. Díaz, M. A. et al. Human-in-the-loop optimization of wearable robotic devices to improve human-robot interaction: A systematic review. *IEEE Trans. Cybern.* (2022).
15. d'Avella, A., Scano, A., Nocilli, M. & Berger, D. J. Challenges and future directions using muscle synergies for reliable assessment in neurorehabilitation. In *International Conference on NeuroRehabilitation*, 717–720 (Springer, 2024).
16. Cheung, V. C. et al. Muscle synergy patterns as physiological markers of motor cortical damage. *Proc. Natl. Acad. Sci.* **109**, 14652–14656 (2012).
17. Zhao, K., Zhang, Z., Wen, H. & Scano, A. Intra-subject and inter-subject movement variability quantified with muscle synergies in upper-limb reaching movements. *Biomimetics* **6**, 63 (2021).
18. d'Avella, A. et al. Combinations of muscle synergies in the construction of a natural motor behavior. *Nat. Neurosci.* **6** (2003).
19. Zhao, K. et al. Muscle synergies for evaluating upper limb in clinical applications: A systematic review. *Heliyon* **9** (2023).
20. Ting, L. H. et al. Neuromechanical principles underlying movement modularity and their implications for rehabilitation. *Neuron* **86**, 38–54 (2015).
21. Langlois, K. et al. Improved motion classification with an integrated multimodal exoskeleton interface. *Front. neurorobot.* 140 (2021).
22. Van Damme, M. et al. Proxy-based sliding mode control of a planar pneumatic manipulator. *Int. J. Rob. Res.* **28**, 266–284 (2009).
23. Úbeda, A. et al. Estimation of neuromuscular primitives from EEG slow cortical potentials in incomplete spinal cord injury individuals for a new class of brain-machine interfaces. *Front. Comput. Neurosci.* **12**, 3 (2018).
24. Gonzalez-Vargas, J. et al. A predictive model of muscle excitations based on muscle modularity for a large repertoire of human locomotion conditions. *Front. Comput. Neurosci.* **9**, 114 (2015).
25. Chvatal, S. A. & Ting, L. H. Common muscle synergies for balance and walking. *Front. Comput. Neurosci.* **7**, 48 (2013).
26. Cheung, V. C. et al. Plasticity of muscle synergies through fractionation and merging during development and training of human runners. *Nat. Commun.* **11**, 4356 (2020).
27. Díaz, M. A. et al. Assessing the influence of robot-assisted movement through muscle synergies similarities. In *10th IEEE RAS/EMBS International Conference for Biomedical Robotics and Biomechatronics (BioRob)*, 1784–1789 (IEEE, 2024).
28. Geng, Y. et al. Modulation of muscle synergies for multiple forearm movements under variant force and arm position constraints. *J. Neural Eng.* **17**, 026015 (2020).
29. Wang, J. et al. Self-adaptive particle swarm optimization with human-in-the-loop for ankle exoskeleton control. *Sens. Mater.* **33** (2021).

Acknowledgements

The authors would like to thank the study participants.

Author contributions

M.D., S.B., K.P., and T.V. conceptualize the study. M.D., S.B., P.M., K.L., and J.W. designed the experiments. M.D., P.M., conducted the experiments. M.D. analyzed muscle activation and synergies data. M.D., S.B,

and T.V. interpreted the data. M.D., P.M and K.P. prepared the initial manuscript. All authors reviewed the manuscript.

Funding
This work was supported by BOSA FOD AI-Driven Wearable Robotics for Healthcare (Aidwear) and the Strategic Research Program Exercise and the Brain in Health and Disease: The Added Value of Human-Centered Robotics, Vrije Universiteit Brussel, Belgium. Kevin Langlois is a postdoctoral fellow of the Research Foundation Flanders (FWO) with FWO grant 1258523N.

Declarations

Competing interests
The authors declare no competing interests.

Additional information
Supplementary Information The online version contains supplementary material available at https://doi.org/10.1038/s41598-025-92611-7.

Correspondence and requests for materials should be addressed to M.A.D. or K.P.

Reprints and permissions information is available at www.nature.com/reprints.

Publisher's note Springer Nature remains neutral with regard to jurisdictional claims in published maps and institutional affiliations.